



OPEN

Estimation of genotoxicity, apoptosis and oxidative stress induction by TiO_2 nanoparticles and acrylamide subacute oral coadministration in mice

Gehan Safwat², Amira A. Mohamed² & Hanan R. H. Mohamed¹✉

Acrylamide is used in the industry and can be a by-product of high-temperature food processing which has toxic potential in various tissues, and titanium dioxide nanoparticles (TiO_2 NPs) are widely used in toothpaste, sweets, food preservation, chewing gum and medicines. Consequently, humans are daily exposed to large amounts of acrylamide and TiO_2 NPs mainly through food intake. However, limited studies are available on the effect of simultaneously intake of acrylamide and TiO_2 NPs on the integrity of genomic DNA and the induction of apoptosis in brain tissues. Therefore, this study estimated the influence of acrylamide coadministration on TiO_2 NPs induced genomic instability and oxidative stress in the brain tissues of mice. To achieve this, mice were orally administrated acrylamide (3 mg/kg b.w) or/and TiO_2 NPs (5 mg/kg b.w) for two successive weeks (5 days per week). The comet assay results showed that concurrent oral administration of acrylamide and TiO_2 NPs strongly induced single- and double stranded DNA breaks, and that the level of reactive oxygen species (ROS) was also highly elevated within neural cells after simultaneous oral intake of acrylamide and TiO_2 NPs compared to those observed after administration of acrylamide or/ TiO_2 NPs alone. Moreover, oral co-administration of acrylamide with TiO_2 NPs increased apoptotic DNA damage to neurons by upregulating the expression levels of P53, TNF- α , IL-6 and Presenillin-1 genes compared to groups administered TiO_2 NPs. Therefore, from these results, the present study concluded that coadministration of acrylamide renders TiO_2 NPs more genotoxic and motivates apoptotic DNA damage and oxidative stress induced by TiO_2 NPs in brain cells, and thus it is recommended to avoid concurrent oral acrylamide administration with TiO_2 NPs.

The effect of nanoparticles on human health has recently been the subject of much controversy. A total of 1814 nanotechnology-based items have been supplied to the global market, of which 117 are classified under the “Food and Beverage” category, according to the Nanotechnology Consumer Product Inventory¹. Titanium dioxide nanoparticles (TiO_2 NPs) are one of the nanoparticles widely used in the preservation of foods and various consumer products such as sweets, chewing gum and cosmetics. TiO_2 NPs are also used as food additives in many food products such as skimmed milk, cheeses, pastries, ice-creams, and sauces²⁻⁴.

As a result of these intensive uses human daily ingestion of TiO_2 NPs is increased through oral intake of various foods and products containing TiO_2 NPs. Scientific interests in studying the bio-distribution and toxicities of TiO_2 NPs are growing. Several in vivo studies have demonstrated the distribution and entrance of TiO_2 NPs to the liver, kidney, lung, and even the brain by crossing the blood-brain barrier^{2,5-7}. Upon entry, TiO_2 NPs attack and destroy the cell genome resulting in chromosomal abnormalities, DNA breakage and genes' mutation leading to apoptosis^{3,6,8,9}.

Many toxic substances other than nanoparticles are also ingested by humans as a result of food processing and heat treatments that cause chemical transformation of food components. Examples for food-processing-induced toxins heterocyclic aromatic amines, advanced glycation end products, nitrosamines, and acrylamide. Acrylamide

¹Zoology Department Faculty of Science, Cairo University, Giza, Egypt. ²Faculty of Biotechnology, October University for Modern Sciences and Arts, Giza, Egypt. ✉email: hananeyra@cu.edu.eg

is a colorless and odorless by-product formed when foods containing high levels of carbohydrates and asparagine molecules are roasted at a certain temperature. A notable example of treatment-induced toxins is acrylamide^{10,11}.

During high temperatures, above 120 °C, and low humidity, the amino acid asparagine reacts with reducing sugars such as glucose and fructose to form acrylamide. Acrylamide can be found in fried, baked and grilled dishes in the highest concentrations¹². Clastogenicity and genotoxicity of acrylamide have been demonstrated in different experimental systems as manifested by the induction of chromosomal aberrations, DNA damage and mutations observed in mice and rats after administration of acrylamide¹³⁻¹⁸.

However, too limited studies are available on the effect of coadministration of acrylamide with TiO₂NPs on the genomic DNA integrity and reactive oxygen species (ROS) generation in the brain tissues of mice. Thus, the current study was undertaken to estimate the impact of acrylamide concurrent administration with TiO₂NPs on the genomic DNA integrity and oxidative stress induction in the brain tissue of mice. Alkaline comet and ladder DNA fragmentation assays was conducted to assess the integrity of genomic DNA. The levels of apoptotic genes expression and intracellular ROS were also studied using quantitative real time polymerase chain reaction (qRT-PCR) and 2,7 dichlorofluorescin diacetate dye, respectively.

Materials and methods

Chemicals. Acrylamide was purchased in the form of white powder from Sigma-Aldrich Chemical Company (St. Louis, MO, USA) and dissolved in deionized distilled water to prepare the administrated dose 3 mg/kg b.w that equivalent to human exposure dose¹⁹. Likewise, TiO₂NPs was obtained in the form of white powder from Sigma-Aldrich Chemical Company (St. Louis, MO, USA) with particle size less than 100 nm and freshly suspended using ultra-sonication in deionized distilled water instantly before use to prepare the tested dose (5 mg/kg b.w) of TiO₂NPs^{20,21} that equivalent to human exposure dose. The other used chemicals and reagents in the experiments were of analytical and molecular biology grade.

Characterization of TiO₂NPs. The purchased TiO₂NPs with a purity of 99.5% and CAS number 13463-67-7 was well characterized using X-ray diffraction (XRD) to ensure the purity of the crystalline TiO₂NPs and also the shape and average particle size of the suspended TiO₂NPs were studied using transmission electron microscopy (TEM).

Animals. Male Swiss Webster mice (20–25 g) were purchased from Animal House of the National Organization for Drug Control and Research (NODCAR), Giza, Egypt and were left for one week before treatment under a standard light–dark cycle to acclimatize to animal house conditions (12-h light cycle, 25 ± 2 °C temperature) with free access to standard rodent chow and water at the Department of Zoology, Faculty of Science, Cairo University.

Ethical approval. The protocol and experimental design of this study have been reviewed and approved by the Institutional Animal Care and Use Committee (IACUC) at Cairo University with the accreditation number (CU/I/F/15/18). This study was reported according to ARRIVE guidelines and also Animal handling and experimentations were conducted in accordance with the Guidelines of the National Institutes of Health (NIH) regarding the care and use of animals for experimental procedures.

Ethical approval for animals. This study was reported according to ARRIVE guidelines and the protocol and experimental design of this study have been reviewed and approved by the Institutional Animal Care and Use Committee (IACUC) at Cairo University with the accreditation number (CU/I/F/15/18).

Experimental design

Twenty four male mice were randomly divided into four groups; each group contained six animals: the first group (Group I) was the negative control group in which the mice were orally given deionized distilled water. The second group (Group II) mice were given orally acrylamide at the exposure dose level of 3 mg/kg body weight¹⁹, while in the third group (Group III) mice were given orally 5 mg/kg body weight of TiO₂NPs^{20,21} that equivalent to human exposure dose. Finally, acrylamide (3 mg/kg b.w) and TiO₂NPs (5 mg/kg b.w) were orally coadministered to mice of Group IV simultaneously. Acrylamide or/and TiO₂NPs were administered five times per week for two successive weeks and 24 h after the last administration the mice were sacrificed and dissected to obtain brain tissues, then stored at – 80 °C for further molecular studies.

Alkaline comet assay to assess DNA breakages. The induction of DNA damage in the brain tissues of four groups was studied using alkaline Comet assay based on the protocol of Tice et al.²². About 100 mg of brain tissues were gently homogenized and 10 µl of clear suspensions containing about 10,000 cultured cells were mixed with 80 µl of 0.5% low melting point agarose. This mixture was then spread on a fully frosted slide which was fully pre-dipped in normal melting agarose (1%). After drying and hardening, the slides were placed in cold lysis buffer with freshly added 10% DMSO and 1% Triton X-100 for 24 h at 4°C in darkness. Slides were then dipped in a freshly prepared alkaline buffer for 15 min and electrophoresed single-stranded DNA for 30 min at 25 V and 300 mA (0, 90 V/cm). The slides were neutralized in 0.4 M Trizma base (pH 7.5) to neutralize the alkali, fixed in absolute cold ethanol, left to air dry and finally, slides were stored at room temperature until they imaged and scored. For scoring slides were immediately stained with ethidium bromide (2 µg/ml) prior imaging, examined and photographed using epi-fluorescent microscope. The DNA migration for each sample was determined by simultaneous image capturing and scoring of 50 cells for each sample using TriTek Comet ScoreTM Freeware

Gene	Strand	Sequence
P53	Forward	5'ACC ATC GGA GCA GCC CTC AT 3'
	Reverse	5'TAC TCT CCT CCC CTC AAT AAG 3'
TNF- α	Forward	5'CCC GAG TGA CAA GCC TGT AG 3'
	Reverse	5'GAT GGC AGA GAG GAG GTT GAC 3'
IL-6	Forward	5'CAT GTT CTC TGG GAA ATC GTGG 3'
	Reverse	5'AAC GCA CTA GGT TTG CCG AGTA 3'
Presenillin-1	Forward	5' AAA GGT CCA CTT CGA CTC CA 3'
	Reverse	5' GGC ATT CCT GTG ACA AAC AA 3'
β -actin	Forward	5'TCA CCC ACA CTG TGC CCA TCT ACGA 3'
	Reverse	5'GGA TGC CAC AGG ATT CCA TAC CCA 3'

Table 1. Sequences of the used primers in qRT-PCR.

v1.5 scoring software that demonstrated some of the function of the Auto Comet(tm). Tail length, % DNA in tail and tail moment were used as indicators for the DNA in neural cells.

Ladder DNA fragmentation assay. Induction of apoptotic DNA damage by acrylamide or/ and TiO₂NPs was studied using ladder DNA fragmentation assay because DNA fragmentation is considered as one of the later steps in the apoptotic process. Using Sriram et al.,²³ protocol: about 50 mg of brain tissues was homogenized in Tris EDTA (TE) lysis buffer containing 0.5% sodium dodecyl sulfate and 0.5 mg/ml RNase A, and then incubated at 37 °C for 1 h. Added Proteinase K (0.2 mg/ml), incubated the samples at 50 °C overnight, and DNA was then extracted and precipitated. The extracted DNA was electrophoresed in 1% agarose gel at 70 V and visualized using a UV trans-illuminator and photographed.

Studying the intracellular ROS generation. Effect of acrylamide or/ and TiO₂NPs administration on the level of intracellular ROS generation was studied using 2,7 dichlorofluorescin diacetate dye. This dye passively enters within cells and interacts with ROS forming the highly fluorescent compound dichlorofluorescein²⁴. An equal volume of cells suspension and 2,7 dichlorofluorescin diacetate dye were gently mixed and incubated for 30 min in dark. Then this mixture was layered and spread on clean slide, and the cells were visualized and photographed using epi-fluorescence microscope at 20 \times magnification.

Measuring the expression levels of p53, IL-6, TNF- α and presenillin-1 genes. Quantitative Real Time Polymerase Chain Reaction (qRT-PCR) was conducted to estimate the effect of acrylamide or/and TiO₂NPs administration on the expression levels of p53, Interleukin-6 (IL-6), Tumor necrosis factor- α (TNF- α), and Presenillin-1 genes in brain tissues of the control and treated groups. Whole cellular RNA was first extracted from brain tissue using Gene JET RNA Purification Kit and using the Nanodrop device the purity and concentration of the total extracted RNA were measured. Based the instructions of Revert Aid First Strand cDNA Synthesis Kit total extracted RNA was completely converted into complementary DNA (cDNA). For measuring the expression levels of P53, IL-6, TNF-alpha and Presenillin-1 genes a separate SYBR green based qRT-PCR was done for each sample using the previously designed primers shown in Table 1^{25,26}. Duplicate of each group were done for each gene and the results of gene expression were normalized to β -actin as a housekeeping gene. Gene expression was quantified using the comparative Ct (DDCt) method and the fold values calculated using the formula: $x = 2^{(-\Delta\Delta Ct)}$.

Statistical analysis. Results of the current study are expressed as mean \pm Standard Deviation (S.D) and were analyzed using the Statistical Package for the Social Sciences (SPSS) (version 20) at the significance level $p < 0.05$. One way analysis of variance (ANOVA) followed by Duncan's test was used to compare between the different treated groups and untreated control group.

Results

Characterization of TiO₂NPs. The obtained XRD pattern confirmed the purity of TiO₂NPs as manifested from the appearance of the characteristic bands of TiO₂NPs at angles of 25.2°, 27.8°, 36.1°, 41.2° and 54.7° shown in Fig. 1. Imaging with TEM revealed the polyhedral morphology of the suspended TiO₂NPs with an average particle size of 60 nm (Fig. 2).

Induction of DNA breaks. As displayed in Table 2 oral administration of either acrylamide (3 mg/kg b.w) or TiO₂NPs (5 mg/kg b.w) separately resulted in statistically significant increases in the tail length, %DNA in tail and tail moment compared to the negative control values. Furthermore, simultaneous co-administration of acrylamide with TiO₂NPs caused a sudden DNA damage induction as determined by the high statistically significant increases in tail length, %DNA in tail and tail moment as compared to the negative control and TiO₂NPs administered groups. The different degrees of DNA damage noticed in the brain tissues of both negative control and acrylamide or/ and TiO₂NPs administered groups are shown in Fig. 3.

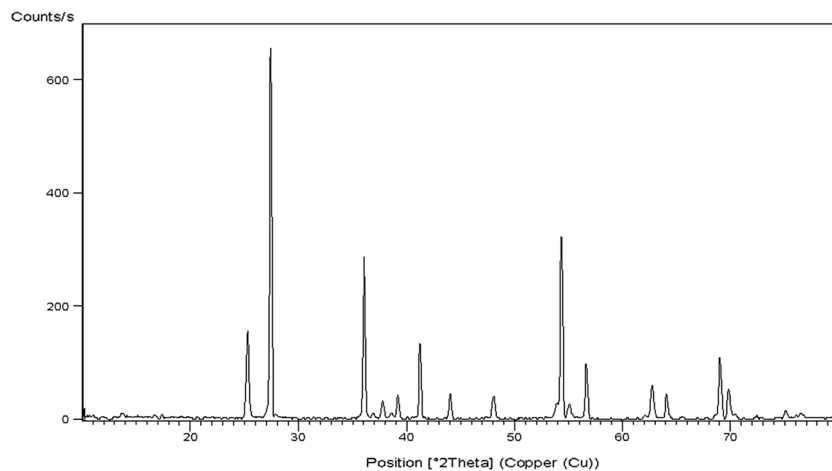


Figure 1. X-Ray Diffraction pattern (XRD) of TiO_2 NPs.

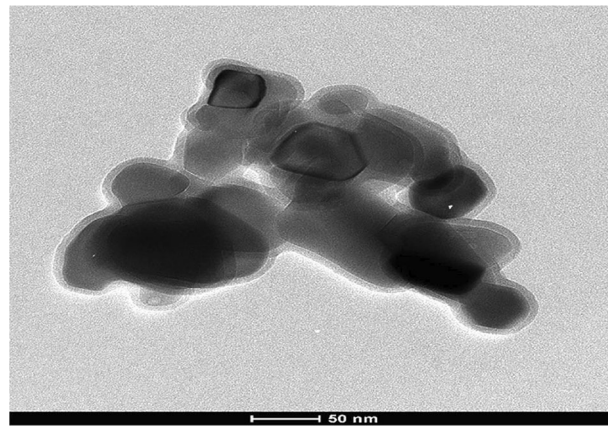


Figure 2. Transmission electron microscope imaging of TiO_2 NPs.

Group	Treatment (dose mg/kg)	Tail length (px)	%DNA in tail	Tail moment
I	Negative control (deionized water)	$3.93 \pm 0.51^{\text{a}}$	$10.18 \pm 1.23^{\text{a}}$	$0.42 \pm 0.03^{\text{a}}$
II	Acrylamide (3 mg/kg)	$7.12 \pm 0.43^{\text{b}}$	$17.73 \pm 1.68^{\text{b}}$	$1.27 \pm 0.04^{\text{b}}$
III	TiO_2 -NPs (5 mg/kg)	$9.09 \pm 0.87^{\text{c}}$	$26.45 \pm 3.32^{\text{c}}$	$2.42 \pm 0.30^{\text{c}}$
IV	Acrylamide + TiO_2 -NPs	$10.43 \pm 1.70^{\text{c}}$	$35.12 \pm 2.90^{\text{d}}$	$3.64 \pm 0.31^{\text{d}}$
One Way Analysis of Variance		F = 23.05 P < 0.001	F = 57.74 P < 0.001	F = 126.39 P < 0.001

Table 2. Tail length (px), %DNA in tail and tail moment in the brain tissue of the negative control group and groups administered acrylamide or/and TiO_2 NPs. Results are expressed as mean \pm SD. Results were analyzed using one-way analysis of variance followed by Duncan's test to test the similarity between the control and three treated groups. Means with different letters indicates statistical significant difference between the compared groups in the same column.

Ladder DNA fragmentation assay. Screening the pattern of the electrophoresed genomic DNA on an ethidium bromide stained agarose gel demonstrated the induction of apoptotic DNA fragmentation by oral administration of acrylamide or/and TiO_2 NPs as manifested by the fragmentized and smeared appearance of the extracted genomic DNA from the brain tissues of mice given acrylamide or/and TiO_2 NPs compared with the intact appearance of genomic DNA extracted from rain tissue of control mice (Fig. 4).

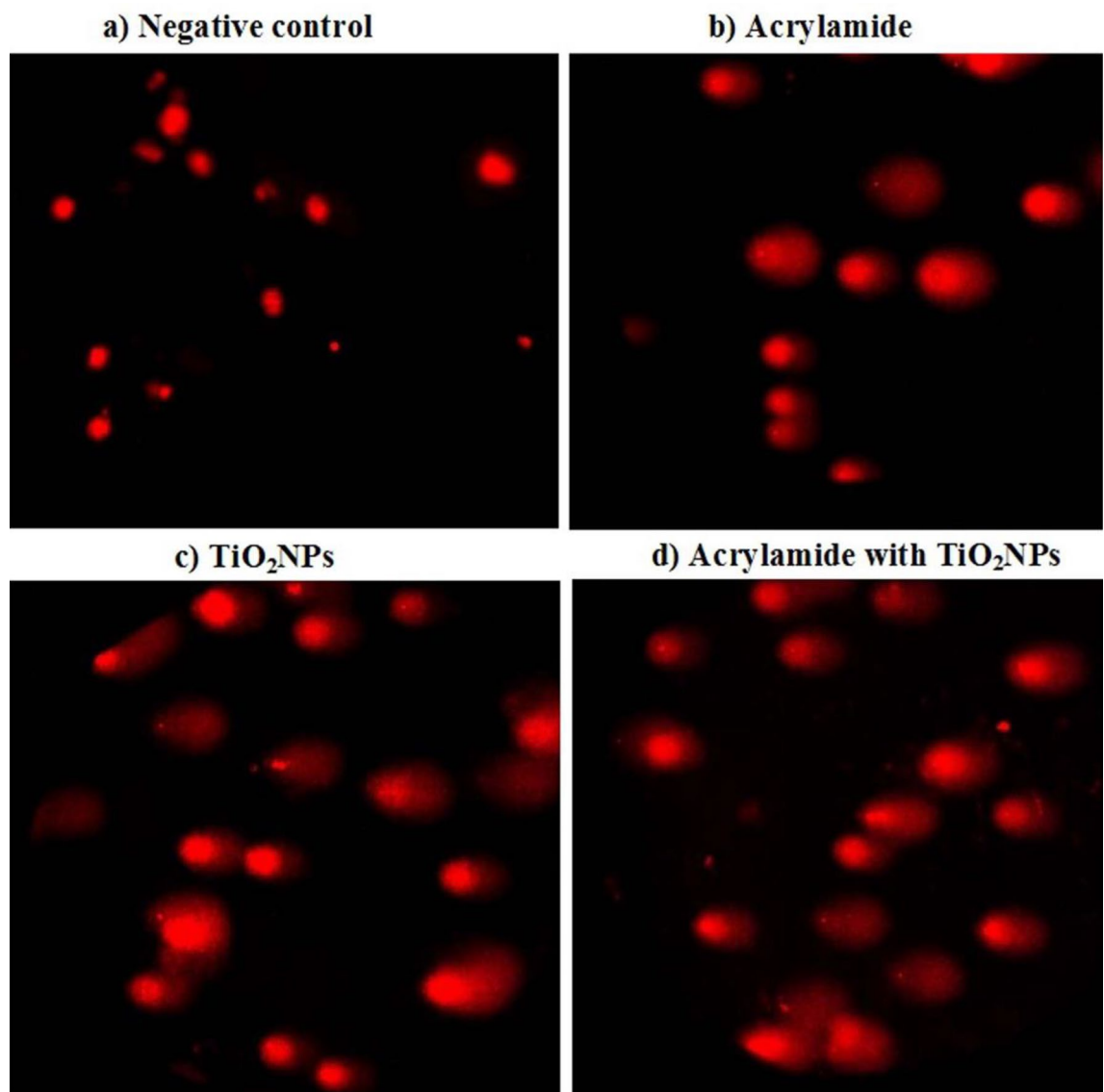


Figure 3. Representative photomicrograph for the observed comet nuclei in the brain tissues of (a) negative control group, (b) acrylamide administrated group, (c) TiO_2 NPs administrated group, and (d) group administered acrylamide with TiO_2 NPs.

Level of intracellular ROS generation. As shown in Fig. 5, the high elevations induced in the ROS generation within neural cells by oral administration of either acrylamide or/and TiO_2 NPs were displayed by the observed high observable increases in the intensity of fluorescent light emitted from the stained neurons compared to that emitted from stained negative control cells. Moreover, concurrent administration of acrylamide with TiO_2 NPs induced marked increases in intracellular ROS generation as indicated by observed remarkable increases in the intensity of emitted fluorescent light emitted compared to that emitted from neural cells of mice given emitted TiO_2 NPs alone (Fig. 5).

Genes' expression. As obvious in Table 3 oral administration of either acrylamide at the dose level 3 mg/kg or TiO_2 NPs at the dose level 5 mg/kg highly upregulated the expression levels of P53, TNF- α , IL-6 and Presenillin-1 genes compared to their expression levels in the negative control group. Furthermore, simultaneous co-administration of acrylamide with TiO_2 NPs significantly increased the expression level of P53, TNF- α , and IL-6 genes, and slightly increased the Presenillin-1 gene expression level compared to their expression levels in mice orally given TiO_2 NPs alone (Table 3).

Discussion

Acrylamide is a common chemical found in molecular biology labs as well as a wide range of manufacturing and processing operations. For example, food cooked at high temperatures forms acrylamide thereby humans are exposed to acrylamide with widely used TiO_2 NPs in a variety of ways through their nutrition, work, leisure

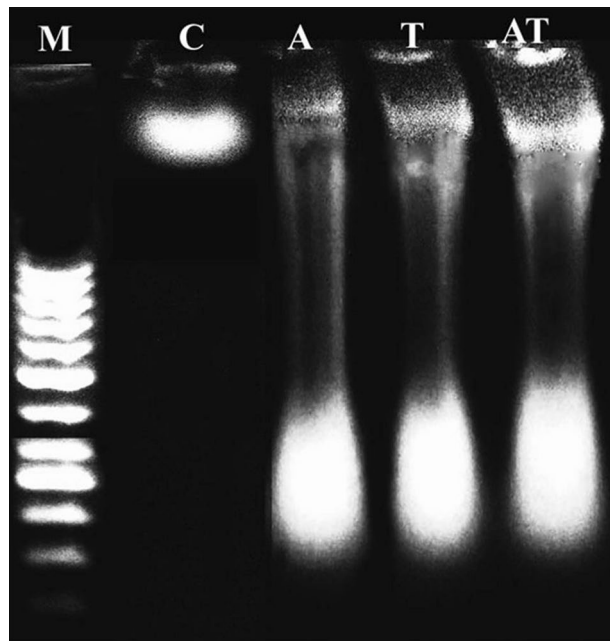


Figure 4. Electrophoresis pattern of the extracted genomic DNA from the negative control group (C) and groups administrated acrylamide (A), TiO₂NPs (T), and acrylamide with TiO₂NPs (AT) on an ethidium bromide stained agarose gel. M: Marker.

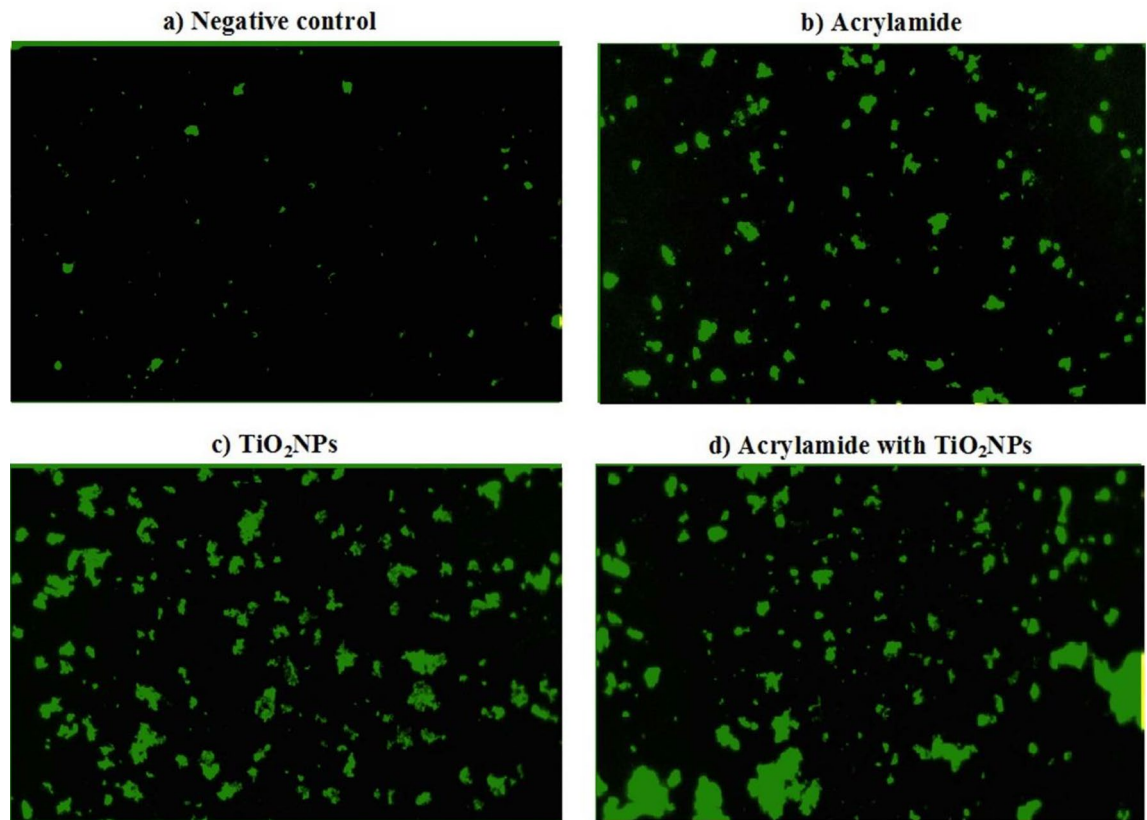


Figure 5. Level of intracellular ROS generation in the brain tissues of (a) negative control group, (b) acrylamide administered group, (c) TiO₂NPs administered group and (d) group administered acrylamide with TiO₂NPs.

Group	Treatment (dose mg/kg)	p53	TNF- α	IL-6	Presenillin-1
I	Negative control (deionized water)	1.00 \pm 0.00 ^a			
II	Acrylamide (3 mg/kg)	4.23 \pm 0.28 ^b	2.71 \pm 0.14 ^b	3.35 \pm 0.11 ^b	2.32 \pm 0.07 ^b
III	TiO ₂ -NPs (5 mg/kg)	2.12 \pm 0.18 ^c	2.06 \pm 0.15 ^c	2.36 \pm 0.07 ^c	1.94 \pm 0.16 ^c
IV	Acrylamide + TiO ₂ -NPs	4.75 \pm 0.24 ^d	3.59 \pm 0.17 ^d	5.26 \pm 0.23 ^d	2.22 \pm 0.10 ^b
One Way Analysis of Variance		F = 214.55 P < 0.001	F = 215.37 P < 0.001	F = 541.18 P < 0.001	F = 105.51 p < 0.001

Table 3. Expression level of p53, TNF- α , IL-6 and Presenillin-1 in the brain tissue of the negative control group and groups administered acrylamide or/and TiO₂NPs. Results are expressed as mean \pm SD. Results were analyzed using one-way analysis of variance followed by Duncan's test to test the similarity between the control and three treated groups. Means with different letters indicates statistical significant difference between the compared groups in the same column.

activities, and other daily routines and surroundings^{27,28}. However, the impact of acrylamide coadministration with TiO₂NPs on genomic integrity and apoptosis induction in brain tissue has not been well studied. Therefore, this study was conducted to estimate the influence of acrylamide coadministration on TiO₂NPs induced genomic instability and apoptosis in mice brain tissue.

According to the results of the comet assay, the current study found that multiple oral administrations of either acrylamide (3 mg/kg b.w) or TiO₂NPs (5 mg/kg b.w) exposure dose caused high DNA breakages as manifested by the remarkable statistically significant increase observed in comet parameters: tail length, %DNA in tail and tail moment compared to negative control values. These results confirmed the DNA damage induction by acrylamide^{13,15-18} or TiO₂NPs^{2,3,6,8,9} reported in previous studies. Moreover, oral simultaneous coadministration of acrylamide with TiO₂NPs augmented genomic DNA disruption and damage as indicated by the observed remarkable elevations in tail length, %DNA in tail and tail moment compared to their values in mice orally given TiO₂NPs alone.

Acrylamide is completely soluble chemical and can cross blood brain barrier attacking brain cells inducing oxidative stress that weaken brain cells and make it more susceptible to TiO₂NPs induced DNA damage^[29,30]. Oxidative stress induction through extra ROS generation by acrylamide administration was manifested in this study from the high elevations in the intensity of fluorescent light emitted from brain cells stained with 2,7 dichlorofluorescein diacetate dye. Meanwhile, over generation of ROS induced by TiO₂NPs alone within brain cells was augmented by coadministration of acrylamide with TiO₂NPs.

Intracellular ROS are naturally generated during various metabolic processes. However, disturbance of balance between ROS generation and antioxidant defense system inducing oxidative stress²⁹⁻³¹. Excessive ROS generation and DNA breakages trigger apoptosis of brain cells. Apoptosis induction by acrylamide and TiO₂NPs administered separately or in combination was demonstrated by the fragmentized smeared appearance of genomic DNA on an ethidium bromide stained agarose gel in consistence with previous studies^{3,32,33}. Ongoing with the results of ROS generation and DNA damage induction, apoptotic DNA damage induction was increased obviously in the genomic DNA of mice orally co-administrated acrylamide with TiO₂NPs.

Moreover, over generation of ROS demonstrated within the brain cells of mice given acrylamide with TiO₂NPs motivated inflammation through excessive release of pro-inflammatory cytokines^{34,35}. Therefore, motivation of TiO₂NPs induced inflammation in the brain tissue can be attributed to high increases in the expression levels of inflammatory IL-6 and TNF- α cytokines demonstrated after coadministration of acrylamide with TiO₂NPs compared to their expression in mice given acrylamide or TiO₂NPs separately.

In response to a variety of cellular stressors such as oxidative stress, hypoxia, DNA damage, ribonucleotide depletion, and oncogene activation, the tumor suppressor p53 gene is activated and overexpressed motivating apoptosis³⁶⁻³⁹. Consequently, the augmentation of TiO₂NPs induced apoptosis noticed in this study may be due to the high increases demonstrated in the expression level of p53 after coadministration of acrylamide with TiO₂NPs compared to its expression in mice given TiO₂NPs or acrylamide separately.

The classical proinflammatory cytokine interleukin-6 (IL-6) performs crucial functions in the development, differentiation, regeneration, and degeneration of neurons in the nervous system. However, as a molecule, IL-6 has the potential to be both useful and harmful. IL-6 is capable of exerting activities that are diametrically opposed to one another, such as promoting neuronal survival after injury or contributing to neuronal degeneration and cell death in conditions such as Alzheimer's disease. Immune cells, such as macrophages, glial cells, and neurons, are some of the primary places where IL-6 is synthesized^{40,41}. Several neural diseases such as Alzheimer's, Parkinson's and Huntington's diseases, brain cancer and ischemic stroke have all been linked to elevated IL-6 expression and secretion. Previous studies have shown that IL-6 is involved in the development of several disorders⁴². Similarly, level of TNF- α gene expression has been shown to elevate in Alzheimer's, and Parkinson's brain tissue, plasma, and cerebrospinal fluid⁴³.

Presenilin1 is encoded by the gene Presenillin-1 and is responsible for the cleavage of the amyloid protein precursor that causes Alzheimer's disease. Presenillin-1 gene has been shown to be overexpressed in Alzheimer's disease⁴⁴. Our finding of high increases in the expression level of presenillin-1 gene after coadministration of acrylamide with TiO₂NPs may be due to the upregulation of IL-6 and TNF- α inflammatory mediators compared to its expression in the brain tissue of mice given TiO₂NPs only. These results are consistent with previous studies^{45,46} that showed that overexpression of inflammatory mediators increase the expression level of β -amyloid

precursor protein and Presenillin-1 genes that cause aggregation and accumulation of β -amyloid peptides in the brain tissues.

Conclusion

Based on the afore discussed results, we concluded that oral simultaneous coadministration of acrylamide motivated TiO_2 NPs induced genomic instability through increasing intracellular ROS generation and the expression level of inflammatory cytokines and tumor suppressor p53 gene. More *in vivo* and *in vitro* studies using fluorescent nanoparticles, electron microscope and mass spectrometry are thus recommended to shed more light on the effect of acrylamide coadministration on TiO_2 NPs induced toxicity in the brain tissue.

Data availability

The datasets used and/or analyzed during the current study are available from the corresponding author on reasonable request.

Received: 7 September 2022; Accepted: 29 October 2022

Published online: 04 November 2022

References

- Baranowska, E., Szwajgier, D. & Oleszczuk, P. Effects of titanium dioxide nanoparticles exposure on human health—A review. *Biol. Trace Elem. Res.* **193**, 118–129 (2020).
- El-Ghor, A. A., Noshy, M. M., Galal, A. & Mohamed, H. R. Normalization of nano-sized TiO_2 -induced clastogenicity, genotoxicity and mutagenicity by chlorophyllin administration in mice brain, liver, and bone marrow cells. *Toxicol. Sci.* **142**(1), 21–32 (2014).
- Mohamed, H. R. H. Estimation of TiO_2 nanoparticle-induced genotoxicity persistence and possible chronic gastritis-induction in mice. *Food Chem. Toxicol.* **83**, 76–83 (2015).
- Dudefou, W., Moniz, K., Allen-Vercoe, E., Ropers, M., & Walker, V. Impact of food grade and nano- TiO_2 particles on a human intestinal community. *Food. Chem. Toxicol.* **106**(Pt A), 242–249 (2017).
- Song, B., Liu, J., Feng, X., Wei, L. & Shao, L. A review on potential neurotoxicity of titanium dioxide nanoparticles. *Nanoscale Res. Lett.* **10**(1), 1042 (2015).
- Mohamed, H. R. H. & Hussien, N. Genotoxicity studies of titanium dioxide nanoparticles (TiO_2 NPs) in the brain of mice. *Scientifica* **2016**, 6710840–47 (2016).
- Mohamed, H. R. H. *et al.* Accumulative persistence of the genotoxic and mutagenic effects induced by low doses of TiO_2 nanoparticles increases the incidence of hepatocellular carcinoma in mice. *Recent Res. Genet. Genom.* **1**(1), 29–47 (2019).
- Trouiller, B., Reliene, R., Westbrook, A., Solaimani, P. & Schiestl, R. H. Titanium dioxide nanoparticles induce DNA damage and genetic instability in vivo in mice. *Cancer Res.* **69**(22), 8784–8789 (2009).
- Shabbir, S., Kulyar, M. F. & Bhutta, Z. A. Toxicological consequences of titanium dioxide nanoparticles (TiO_2 NPs) and their jeopardy to human population. *BioNanoSci.* **11**, 621–632 (2021).
- Dellaflora, L., Dall'Asta, C. & Galaverna, G. Toxicodynamics of mycotoxins in the framework of food risk assessment: An *in silico* perspective. *Toxins (Basel)* **10**(2), 52 (2018).
- Mills, C., Mottram, D. S. & Wedzicha, B. L. Acrylamide. In *Process Induced Food Toxicants: Occurrence, Formation, Mitigation, and Health Risks* (eds Stadler, R. H. & Lineback, D. R.) 23–50 (Wiley, 2019).
- Tareke, E., Rydberg, P., Karlsson, P., Eriksson, S. & Törnqvist, M. Acrylamide: A cooking carcinogen?. *Chem. Res. Toxicol.* **13**, 517–522 (2016).
- Ansar, S., Siddiqui, N. J., Zargar, S., Ganaie, M. A. & Abudawood, M. Hepatoprotective effect of Quercetin supplementation against Acrylamide-induced DNA damage in wistar rats. *BMC Complement Altern. Med.* **16**(1), 327 (2016).
- Hobbs, C. A. *et al.* Differential genotoxicity of acrylamide in the micronucleus and pig-a gene mutation assays in F344 rats and B6C3F1 mice. *Mutagenesis* **31**, 617–626 (2016).
- Jangir, B. L., Mahaprabhu, R., Rahangade, S., Bhandarkar, A. G. & Kurkure, N. V. Neurobehavioral alterations and histopathological changes in brain and spinal cord of rats intoxicated with acrylamide. *Toxicol. Ind. Health* **32**, 526–540 (2016).
- Shimamura, Y., Iio, M., Urahira, T. & Masuda, S. Inhibitory effects of Japanese horseradish (*Wasabia japonica*) on the formation and genotoxicity of a potent carcinogen, acrylamide. *J. Sci. Food Agric.* **97**, 2419–2425 (2017).
- Algarni, A. A. Genotoxic effects of acrylamide in mouse bone marrow cells. *Caryologia* **71**, 160–165 (2018).
- Hagio, S. *et al.* Effect of sampling time on somatic and germ cell mutations induced by acrylamide in gpt delta mice. *Genes Environ.* **43**, 4 (2021).
- Joint FAO/WHO Expert Committee on Food Additives & World Health Organization. Guidance document for WHO monographs and reviewers evaluating food additives (excluding enzyme preparations and flavouring agents), version 1.0. World Health Organization. <https://apps.who.int/iris/handle/10665/206184> (2016).
- Weir, A. A. TiO_2 Nanomaterials: Human Exposure and Environmental Release. M.Sc thesis. Arizona State University (2011).
- Shahare, B. & Yashpal, M. Toxic effects of repeated oral exposure of silver nanoparticles on small intestine mucosa of mice. *Toxicol. Mech. Methods* **23**(3), 161–167 (2013).
- Tice, R. R. *et al.* Single cell gel/comet assay: guidelines for *in vitro* and *in vivo* genetic toxicology testing. *Environ. Mol. Mutagen.* **35**(3), 206–221 (2000).
- Sriram, M. I., Kanth, S. B. M., Kalishwaralal, K. & Gurunathan, S. Antitumor activity of silver nanoparticles in Dalton's lymphoma ascites tumor model. *Int. J. Nanomed.* **5**, 753–762 (2010).
- Siddiqui, M. A. *et al.* Protective potential of trans-resveratrol against 4-hydroxynonenal induced damage in PC12 cells. *Toxicol. In Vitro Int. J. Publ. Assoc. BIBRA* **24**(6), 1592–1598 (2010).
- Suzuki, A., Tsutomi, Y., Yamamoto, N., Shibutani, T. & Akahane, K. Mitochondrial regulation of cell death: Mitochondria are essential for procaspase 3–p21 complex formation to resist Fas-mediated cell death. *Mol. Cell. Biol.* **19**(5), 3842–3847 (1999).
- Lai, M. C. *et al.* Individual differences in brain structure underpin empathizing systemizing cognitive styles in male adults. *Neuroimage* **61**(4), 1347–1354 (2012).
- Teleanu, D. M., Chircov, C., Grumezescu, A. M., Teleanu, R. I. Neurotoxicity of Nanomaterials: An Up-to-Date Overview. *Nanomaterials (Basel)* **9**(1), 96–110 (2019).
- Cota, P. *et al.* *Acrylamide: A Neurotoxin and a Hazardous Waste* 102607 (IntechOpen, 2022).
- Aboubakr, M., Said, A., Elgendey, F., Anis, A. & Ibrahim, S. Neuroprotective effects of clove oil in acrylamide induced neurotoxicity in rats. *Pak. Vet. J.* **39**, 18–331. <https://doi.org/10.29261/pakvetj/2018.117> (2019).
- Farouk, S. M., Gad, F. A., Almeer, R., Abdel-Daim, M. M., & Emam, M. A. Exploring the possible neuroprotective and antioxidant potency of lycopene against acrylamide-induced neurotoxicity in rats' brain. *Biomed. Pharmacother.* **138**, 111458–65. <https://doi.org/10.1016/j.bioph.2021.111458> (2021).

31. Mohamed, H. R. H. Induction of genotoxicity and differential alterations of p53 and inflammatory cytokines expression by acute oral exposure to bulk- or nano-calcium hydroxide particles in mice "Genotoxicity of normal- and nano-calcium hydroxide". *Toxicol. Mech. Methods.* **31**(3), 169–181 (2021).
32. "Genotoxicity of normal- and nano-calcium hydroxide", *Toxicology Mechanisms and Methods*, 31:3, 169–181
33. Kumar, S. & Rajamani, P. Titanium oxide (TiO₂) nanoparticles in induction of apoptosis and inflammatory response in brain. *J. Nanopart. Res.* **2**, 2. <https://doi.org/10.1007/s11051-015-2868-x> (2015).
34. Ibrahim, M. & Ibrahim, M. Acrylamide-induced hematotoxicity, oxidative stress, and DNA damage in liver, kidney, and brain of catfish (*Clarias gariepinus*). *Environ. Toxicol.* <https://doi.org/10.1002/tox.22863> (2019).
35. Mittal, M., Siddiqui, M. R., Tran, K., Reddy, S. P. & Malik, A. B. Reactive oxygen species in inflammation and tissue injury. *Antioxid. Redox Signal.* **20**(7), 1126–1167. <https://doi.org/10.1089/ars.2012.5149> (2014).
36. Mohamed, H. R. H. Acute oral administration of cerium oxide nanoparticles suppresses lead acetate-induced genotoxicity, inflammation, and ROS generation in mice renal and cardiac tissues. *Biol. Trace Elem. Res.* **200**, 3284–3293 (2022).
37. Chen, M. *et al.* Oxidative stress and immunotoxicity induced by graphene oxide in zebrafish. *Aqua Toxicol.* **174**(1879–1514), 54–60 (2016).
38. Jackson, S. P. & Bartek, J. The DNA-damage response in human biology and disease. *Nature* **461**(7267), 1071–1078 (2009).
39. Ahamed, M., Akhtar, M. J. & Alhadlaq, H. A. Preventive effect of TiO₂ nanoparticles on heavy metal Pb-induced toxicity in human lung epithelial (A549) cells. *Toxicol. In Vitro* **57**, 18–27 (2019).
40. Ahamed, M. *et al.* Co-exposure of Bi₂O₃ nanoparticles and bezo[a]pyrene-enhanced in vitro cytotoxicity of mouse spermatogonia cells. *Environ. Sci. Pollut. Res.* **28**, 17109–17118 (2021).
41. Erta, M., Quintana, A. & Hidalgo, J. Interleukin-6, a major cytokine in the central nervous system. *Int. J. Biol. Sci.* **8**(9), 1254–1266 (2018).
42. Ahamed, M., Akhtar, M. J., Khan, M. A. M. & Alhadlaq, H. A. SnO₂-doped ZnO/reduced graphene oxide nanocomposites: Synthesis, characterization, and improved anticancer activity via oxidative stress pathway. *Int. J. Nanomed.* **16**, 89–104 (2021).
43. Kummer, K. K., Zeidler, M., Kalpachidou, T., Kress, M. Role of IL-6 in the regulation of neuronal development, survival and function. *Cytokine*, **144**, 155582–94 (2021).
44. Maddahi, A., Kruse, L. S., Chen, Q. W., Edvinsson, L. The role of tumor necrosis factor- α and TNF- α receptors in cerebral arteries following cerebral ischemia in rat. *J. Neuroinflammation*, **8**, 107–120 (2011).
45. Yang, W. *et al.* Presenilin1 exerts antiproliferative effects by repressing the Wnt/ β -catenin pathway in glioblastoma. *Cell Commun. Signal.* **18**, 22 (2020).
46. Bates, K. A., Fonte, J., Robertson, T. A., Martins, R. N. & Harvey, A. R. Chronic gliosis triggers Alzheimer's disease-like processing of amyloid precursor protein. *Neuroscience* **113**, 785–796 (2002).
47. Sokolova, A. *et al.* Monocyte chemoattractant protein-1 plays a dominant role in the chronic inflammation observed in Alzheimer's disease. *Brain Pathol.* **19**, 392–398 (2009).

Acknowledgements

Many thanks and appreciation to the Department of Zoology, Faculty of Science, Cairo University, for providing the chemicals and equipment needed to conduct experiments.

Author contributions

H.R.H.M.: designed the study plan and performed the experiments, wrote manuscript and conducted statistical analysis. A.A.M. done experimentations and wrote manuscript. H.R.H.M. and G.S. reviewed the manuscript.

Funding

Open access funding provided by The Science, Technology & Innovation Funding Authority (STDF) in cooperation with The Egyptian Knowledge Bank (EKB). The present work was partially funded by Faculty of Science Cairo University and Faculty of Biotechnology, October University for Modern Sciences and Arts (MSA) Egypt.

Competing interests

The authors declare no competing interests.

Additional information

Correspondence and requests for materials should be addressed to H.R.H.M.

Reprints and permissions information is available at www.nature.com/reprints.

Publisher's note Springer Nature remains neutral with regard to jurisdictional claims in published maps and institutional affiliations.



Open Access This article is licensed under a Creative Commons Attribution 4.0 International License, which permits use, sharing, adaptation, distribution and reproduction in any medium or format, as long as you give appropriate credit to the original author(s) and the source, provide a link to the Creative Commons licence, and indicate if changes were made. The images or other third party material in this article are included in the article's Creative Commons licence, unless indicated otherwise in a credit line to the material. If material is not included in the article's Creative Commons licence and your intended use is not permitted by statutory regulation or exceeds the permitted use, you will need to obtain permission directly from the copyright holder. To view a copy of this licence, visit <http://creativecommons.org/licenses/by/4.0/>.

© The Author(s) 2022